9960–9975 *Nucleic Acids Research, 2017, Vol. 45, No. 17* *Published online 18 July 2017*
doi: 10.1093/nar/gkx641

MAZ induces *MYB* expression during the exit from quiescence via the E2F site in the *MYB* promoter

Josué Álvaro-Blanco[1,†], Katia Urso[2,†], Yuri Chiodo[1,†], Carla Martín-Cortázar[1], Omar Kourani[1], Pablo Gómez-del Arco[2,3,4], María Rodríguez-Martínez[1], Esther Calonge[5], José Alcamí[5], Juan Miguel Redondo[2,4], Teresa Iglesias[6,7] and Miguel R. Campanero[1,4,*]

[1]Department of Cancer Biology, Instituto de Investigaciones Biomédicas Alberto Sols, CSIC-UAM, Madrid 28029, Spain, [2]Gene regulation in cardiovascular remodeling and inflammation group, Centro Nacional de Investigaciones Cardiovasculares, Madrid 28029, Spain, [3]Department of Molecular Biology, Universidad Autónoma de Madrid, Centro de Biología Molecular, Cantoblanco, Madrid 28049, Spain, [4]CIBERCV, Spain, [5]Unidad de Inmunopatología del SIDA, Centro Nacional de Microbiología, Majadahonda 28220, Spain, [6]Department of Endocrine and Nervous Systems Pathophysiology, Instituto de Investigaciones Biomédicas Alberto Sols, CSIC-UAM, Madrid 28029, Spain and [7]CIBERNED, Centro de Investigación Biomédica en Red sobre Enfermedades Neurodegenerativas, Spain

Received September 22, 2016; Revised July 08, 2017; Editorial Decision July 11, 2017; Accepted July 13, 2017

ABSTRACT

Most E2F-binding sites repress transcription through the recruitment of Retinoblastoma (RB) family members until the end of the G1 cell-cycle phase. Although the *MYB* promoter contains an E2F-binding site, its transcription is activated shortly after the exit from quiescence, before RB family members inactivation, by unknown mechanisms. We had previously uncovered a nuclear factor distinct from E2F, Myb-sp, whose DNA-binding site overlapped the E2F element and had hypothesized that this factor might overcome the transcriptional repression of *MYB* by E2F-RB family members. We have purified Myb-sp and discovered that Myc-associated zinc finger proteins (MAZ) are major components. We show that various MAZ isoforms are present in Myb-sp and activate transcription via the *MYB*-E2F element. Moreover, while forced RB or p130 expression repressed the activity of a luciferase reporter driven by the *MYB*-E2F element, co-expression of MAZ proteins not only reverted repression, but also activated transcription. Finally, we show that MAZ binds the *MYB* promoter *in vivo*, that its binding site is critical for *MYB* transactivation, and that *MAZ* knockdown inhibits *MYB* expression during the exit from quiescence. Together, these data indicate that MAZ is essential to bypass *MYB* promoter repression by RB family members and to induce *MYB* expression.

INTRODUCTION

The proto-oncogene *MYB* was initially identified as a frequent integration site for avian and murine retroviruses, leading to a range of leukemias (1). In addition, *MYB* overexpression was found in several other cancer types, including neuroblastoma, melanoma, glioblastoma and neoplasias from colon, pancreas and breast (2,3). *MYB* encodes a sequence-specific DNA-binding transcriptional regulator that is highly expressed in embryonic nervous system, liver, kidney and colon mucosa. In the adult, its expression levels are high in epithelial progenitor cells in colon crypts; hematopoietic progenitors; activated mature T and B lymphocytes; and ependymal cells, progenitor cells and some neuroblasts located at neurogenic regions in the subventricular zone of adult brain (2,3). MYB, also known as proto-oncogene C-MYB, plays a central role in the regulation of hematopoietic cell development, and the control of its expression is critically important in cell proliferation and differentiation of both normal and tumor cells. Indeed, *MYB* anti-sense oligonucleotides inhibit cell proliferation and its forced expression blocks cell differentiation (3,4). In addition, the analysis of *Myb*-targeted mice demonstrated a critical role for Myb in fetal hematopoiesis and colon development (1,3).

In normal cells, *MYB* expression is tightly regulated at transcriptional and post-transcriptional levels. However, in spite of its critical relevance, the regulation of *MYB* expression is not well understood. *MYB* is not expressed in quiescent cells, but its transcription is promoted shortly after the stimulation of cell proliferation. Its promoter lacks canonical TATAA and CAAT boxes, but harbors several GC boxes and binding sites for various transcriptional reg-

*To whom correspondence should be addressed. Tel: +34 91 5854490; Fax: +34 91 5854401; Email: mcampanero@iib.uam.es
†These authors contributed equally to the paper as first authors.

ulators. In particular, the human and mouse promoters contain a binding site for members of the E2F family of transcriptional regulators (5,6). This family plays a central role in cell cycle regulation by restricting genes expression to the precise time of the cell cycle in which their products are required (7). Most E2F factors are composed of two subunits, termed E2F and declustering potential (DP), which form heterodimeric complexes. Eight *E2F* genes (*E2F1-E2F8*) and two *DP* genes (*DP1* and *DP2*) are expressed in mammals. The Retinoblastoma tumor suppressor protein (RB) and its family members p107 and p130 bind to E2F factors and block their transactivation capacity. The recruitment of RB family members to gene promoters exerts a dominant negative effect on their transcription due to the association of RB and its family members with chromatin remodelers (8,9). The RB family member p130 is particularly essential, as a component of the *dimerization partner, RB-like, E2F and multi-vulval class B* (DREAM) complex, for repression of E2F-regulated genes in quiescent cells (9,10). RB family members are inactivated by phosphorylation mediated by cyclin-dependent kinases (CDKs) at the G1-S boundary and thus release E2F repressors from promoters and enable transcriptional activation (7). As a consequence, most genes that contain E2F elements are not transcriptionally activated before the G1-S transition. *MYB*, however, is an exception to this rule; although *MYB* contains an E2F element and can be induced by forced E2F1 expression (6), its induction occurs early after the exit from quiescence (11,12), before RB family inactivation and remains constitutive in subsequent cell cycles (12). These results indicated that *MYB* is able to escape from the dominant transcriptional repression of E2F–RB family complexes during specific times of G1.

We hypothesized that the interaction of proteins distinct from E2F with the *MYB*-E2F site might account for the early activation of its promoter. We had previously discovered a nuclear factor, referred to as Myb-sp, that contained no E2F/DP or RB family members and specifically interacted with the *MYB*-E2F site, but not with the E2F element from other promoters (5). However, the identity of this factor remained elusive. Here we have identified Myc-associated zinc finger proteins (MAZ) as major components of Myb-sp and demonstrated their capacity to overcome transcriptional repression by RB family members through the *MYB*-E2F element. We also show that MAZ proteins are essential mediators of *MYB* induction during the exit from quiescence.

MATERIALS AND METHODS

Cell culture and preparation of nuclear extracts and *in vitro*-translated proteins

DG-75 and Jurkat cells were grown in RPMI 1640 medium, whereas Saos-2 and human embryonic kidney 293T (HEK-293T) cells were grown in Dulbecco's modified Eagle's medium. Both media were supplemented with 10% fetal bovine serum (FBS), penicillin, streptomycin and L-glutamine. All cells were maintained at 37°C in a humidified 5% CO_2-containing atmosphere. Buffy coats of healthy individuals were obtained from the Madrid Blood Donor Centre (Madrid, Spain). Human peripheral blood lymphocytes (PBLs) were isolated from buffy coats as described previously (13) and then stimulated with 5 μg/ml leucoagglutinin (L4144; Sigma-Aldrich, Madrid, Spain) and cultured in RPMI 1640 medium supplemented with 10% FBS, penicillin, streptomycin, L-glutamine and 50 U/ml of human recombinant interleukin 2 (IL2) (14). Cell cycle synchronization of lymphocytes was done as described (15). Briefly, after 12 days, blast cells were turned quiescent by transferring them to medium without IL2 and 2 days later cells were induced to exit quiescence by stimulation with 5 μg/ml leucoagglutinin plus 50 U/ml of IL2. Institutional Review Board approval was obtained for these studies and all participants provided written informed consent. Nuclear extracts were prepared as previously reported (16). pcDNA3-HA-MAZ-1 or -MAZ-2s were *in vitro* transcribed and translated by using TnT® coupled reticulocyte lysate systems (L-4610; Promega, Madison, WI, USA) following manufacturer recommendations.

Antibodies and immunoblotting

The anti-MAZ MAZ-N12, MAZ-C13, MAZ-C2 and MAZ-123 polyclonal rabbit sera were raised against KLH-conjugated peptides derived from the amino- or carboxy-terminal regions of Human MAZ proteins. Antibodies against HA (MMS-101P), SMAD2/3 (sc-6032x) and Tubulin (T9026) were purchased from Covance (Covance), Santa Cruz (Santa Cruz, CA, USA) and Sigma-Aldrich, respectively. The anti-DP1 polyclonal rabbit antibody was described previously (5). For immunoblotting, we used antibodies to MAZ, MAZ phospho-S460 (sc-16318, Santa Cruz), E2F1 (sc-193x, Santa Cruz), pRB (554136, BD Biosciences Pharmingen), p130 (sc-374521, Santa Cruz), p130 phospho-S672 (ab76255, Abcam), Tubulin (T9026, Sigma-Aldrich) and a combination of RB phospho-S780, phospho-S795 and phospho-S807/811 (8180, 9301 and 8516 from Cell Signaling), followed by peroxidase-conjugated anti-rabbit (A1949) or anti-mouse (A2304) antibodies (Sigma-Aldrich). Chemiluminescent detection reagent (Perkin-Elmer, Waltham, MA, USA) was used and the membrane exposed to X-Ray Medical film.

Electrophoretic mobility shift analysis

Gel shifts were performed with labeled double-stranded oligonucleotides (Sigma–Aldrich) encompassing the *E2F* elements from the *MYB*, *DHFR* and *CDC2* promoters. The sequences of these oligonucleotides (5′ to 3′) were: *MYB* (CTAGACAGATTTGGCGGGAGG GGGG and GATC CCCCCCTCCCGCCAATCTGT); *DHFR* (CTAGAGCA ATTTCGCGCCA AACTTG and GATCCAAGTTTG GCGCGAAATTCGT); and *CDC2* (CTAGATTTCTTT CG CGCTCTAGCCG and GATCCGGCTAGAGCGC GAAAGAAAT). The top-strand oligonucleotide sequence (5′ to 3′) of the *MYB*-E2F mutants was: *MYB-Sp* (CT AGAC AGATTT**ATA**GGGAGGGGGG), *MYB-E2F* (CT AGACAGATTTGGCGGGAG**AT**GGG) and *MYB-Null* (CTAGACAGATTT**ATA**GGGAG**AT**GGG). Binding reactions were performed in buffer D (BFD) (20 mM HEPES pH 7.9, 20% glycerol, 80 mM KCl, 0.2 mM ethylenedi-

aminetetraacetic acid, 0.5 mM dithiothreitol (DTT)) supplemented with sheared salmon sperm DNA and purified bovine serum albumin (BSA), as described previously (13). Unlabeled oligonucleotide competitors (100 ng) and antibodies (1 μg of purified antibodies or 1 μl of crude polyclonal antibodies) were also added to the initial mix prior to the pre-incubation step. Following pre-incubation, the labeled oligonucleotides were added (1 ng) and the mixtures were incubated for another 20 min at room temperature. Samples were then loaded directly onto a running non-denaturing 4% acrylamide-0.1% bisacrylamide gel at 4°C. Retarded complexes were visualized by autoradiography (1–16 h at room temperature).

UV cross-linking experiments

Ultraviolet (UV) cross-linking of DNA/protein complexes was carried out essentially as described (13). Bromodeoxyuridine (BrdU)-substituted ^{32}P-labeled probes were prepared by annealing the oligonucleotide primer UV-common (5′-GATCCACTGAGCCT-3′) with the E2F-c-myb-UV oligonucleotide (CTAGACAGATTTGGC GG GAGGGGGAGGCTCAGTG-3′). Labeling (200 ng) was achieved by a Klenow fill-in reaction performed for 1–2 h at 4°C with [α-^{32}P]dGTP and [α-^{32}P]dCTP and unlabeled dATP and bromo-dUTP (Sigma-Aldrich) in the labeling reaction. Unincorporated nucleotides were removed by chromatography over Sephadex G25. Electrophoretic mobility shift analyses (EMSAs) were performed with the BrdU-substituted probes as described above except that the binding reaction was scaled-up 2-fold. Immediately after electrophoresis, the wet gel was covered with plastic wrap and exposed to UV light (500 mJ) with a Stratalinker 1800 (Agilent Technologies, Santa Clara, CA, USA). The positions of various complexes were determined by 1–2 h autoradiography at 4°C. Gel slices containing various complexes were excised and soaked in 50–100 μl of 2× sodium dodecyl sulfate (SDS) sample buffer at 65°C for 30 min. The samples were boiled for 5 min and electrophoresed through an SDS-8% polyacrylamide gel along with pre-stained molecular weight markers (BioRad Laboratories, Hercules, CA, USA).

Purification and identification of Myb-sp

DNA affinity columns were prepared. Double-strand oligonucleotides Myb-Sp-ac (5′-CTAGACAGA TTTATAGGGAGGGGGG-3′ and 5′-GATCCC CCCCTCCCTATAAATCTGT-3′) or Myb-Null-ac (5′-CTAGACAGATTTATAGGGAGATGGG-3′ and 5′-GATCCCCATCTCCCTA TAAATCTGT-3′) where subjected to 5′-phosphorylation and concatemerized with DNA ligase. The concatemerized DNA (100 μg) was coupled to 1 ml of cyanogen bromide-activated-Sepharose 4B (17–0430-01, Amersham) and loaded onto columns that were then equilibrated in BFD80 (as BFD except that KCl was used at 80 mM). Nuclear extracts from 109 DG-75 cells were pre-cleared by partial protein precipitation with 25% acetone (2 h at 4°C). Acetone was evaporated during 1 h at 4°C in a vacuum chamber and samples were centrifuged 15 min at 17 000 × *g* at 4°C. Supernatant was dialyzed against BFD80 and then loaded onto a column prepared with Myb-Null-ac-coupled resin. The flow-through was loaded in a column prepared with Myb-Sp-ac-coupled resin and both columns were washed with three volumes of BFD80 supplemented with 1% NP40, two volumes of BFD80, three volumes of BFD150 (as BFD except that KCl was used at 150 mM) and two volumes of BFD80. Bound proteins were eluted with 300 ng/μl of double-strand Myb-Sp-ac oligonucleotides in BFD. All buffers contained 1 mM PMSF, 1 mM Na3VO4 and 1 mM NaF added immediately before use. Eluted proteins were precipitated with 10% tri-chloro-acetic acid and fractionated through 10% sodium dodecyl sulphate-polyacrylamide gel electrophoresis (SDS-PAGE). A silver-stained band at 30 kDa in the Myb-Sp column was excised from the gel, subjected to tryptic digestion and analyzed by mass spectrometry at the proteomics facility of The Spanish National Center for Biotechnology (CNB-CSIC; Madrid, Spain). Bands of interest were trypsin-digested by automated in-gel digestion in a Proteineer DP (Bruker Daltonics). Tryptic peptides were extracted and analyzed by LC-MS/MS using a nano-HPLC system (Eksigent Technologies nanoLC Ultra 1D plus, AB SCIEX) coupled online to a TripleTOF 5600 mass spectrometer (AB SCIEX) with a nano-spray ionization source. The analytical and trap columns were a nano-Acquity UPLC column (1.7 μm, BEH 130 C18; Waters) and a nanoViper column Acclaim PepMap C18, 5 μm (Thermo Fisher Scientific), respectively. The loading pump delivered 0.1% formic acid in water at 2 μl/min; the nanopump provided a flow rate of 250 nl/min and was operated in gradient elution conditions with 0.1% formic acid in water as mobile phase A, and 0.1% formic acid in acetonitrile (ACN) as mobile phase B. Gradient elution was performed as follows: 98% A:2% B for 1 min, a linear increase to 30% B in 110 min and to 40% B in 10 min, then to 90% B in 5 min; isocratic conditions of 90% B for 5 min and return to initial conditions in 2 min. One-third of the sample was processed by nanoLC-MS in a 5-μl injection volume. Settings for TripleTOF were: ionspray voltage floating (ISVF) = 2800 V, curtain gas (CUR) = 20, interface heater temperature (IHT) = 150, ion source gas 1 (GS1) = 30, DP = 85 V. Data were acquired in an information-dependent acquisition (IDA) mode with Analyst TF 1.7 software (AB SCIEX). For IDA parameters, a MS survey scan (250 ms) in the mass range of 350–1250 m/z was followed by 25 MS/MS scans (100 ms) in the mass range of 100–1500 m/z. Switching criteria set to ions greater than m/z = 350 and smaller than m/z = 1250, with a charge state of 2–5, threshold >90 counts (cps) and dynamic exclusion of 20 s. Collision energy (CE) was set as rolling CE using a parameter script.

MS and MS/MS data were processed using Analyst TF 1.7 Software. Raw data were translated to mascot general file (mgf) format using the PeakView program v.1.2 and a Uniprot database (26 March 2014) with human taxonomy restriction (NEWT 9606), containing 39 785 protein-coding genes and their reverse entries in an in-house Mascot Server v.2.5.1 (Matrix Science). Search parameters were as follows: fixed modification of carbamidomethyl cysteine; variable modifications oxidation of methionines and acetylation of the peptide N-termini; peptide mass tolerance ±25 ppm; fragment mass tolerance ±0.05 Da; maximum

of two trypsin digestion missed-cleavages. Typical MS and MS/MS spectra accuracy was ±10 ppm. Criteria to accept individual spectra were based on Mascot ion score threshold (0.05) as the standard ion score threshold, and the identification certainty was established using false discovery rate criteria (FDR ≤ 1%) for peptide and protein matches using the Scaffold bioinformatic tool v.4.2.1 (Proteome Software). This cutoff value for protein identification corresponded to a Mascot score of protein identification of 25. A. The mass spectrometry proteomics data have been deposited to the ProteomeXchange Consortium via the PRIDE (17) partner repository with the dataset identifier PXD006857 and 10.6019/PXD006857.

Construction of vectors

Full-length *MAZ-1*, *MAZ-2* and *MAZ-2s* coding sequences were obtained by polymerase chain reaction (PCR) amplification from cDNA obtained from DG-75 cells and cloned immediately downstream from the HA-tag into pcDNA3 (ThermoFischer Scientific, Waltham, MA USA). PCR primer sequences (5′-3′) were as follows: MAZ-1/2Forward: CTAACGGGATCCATGTTCCC GGTG TTTCCTTGCACGCTGC; MAZ-1Reverse: CTAACGGAATTCTCACCAGGGTTGGGAGGGA AGTGGC; MAZ-2sForward: TTAACGGGATCCAT GGTGCCCCTGAGCCTCCTGAGC; MAZ-2Reverse: TGACTGGAATTCTCAGCAGGTGGGCTGTGGCT GGGGGG. MAZ-1, *MAZ-2* and *MAZ-2s* cDNAs were generated employing, respectively, MAZ-1/2Forward and MAZ-1Reverse, MAZ-1/2Forward and MAZ-2Reverse and MAZ-2sForward plus MAZ-2Reverse.

pBG-LUC was described previously (18) and was generated by cloning the ß-globin TATA box immediately upstream from the luciferase gene in the pGL2-basic plasmid. To generate the wild-type (WT) version of *2xE2F/MAZ-Luc* and its mutant derivatives, the annealed *2xMYB-WT* (CGCGTCAGAT TT**GGC**GGGAG**GG**GGACAGATTT**GGC**GGGAG**GG** GGAA) and (GATCTTCCCCCTCCCGCCAAATCT GTCCCCCTCCCGCCAAATCTGA); *2xMYB-E2F* (CGCGTCAGATTT**GGC**GGGAG**AT**GGACAGAT TT**GGC**GGGAG**AT**GGAA) and (GATCTTCC**AT**CTCC C**GCC**AAATCTGTCC**AT**CTCCC**GCC**AAATCTGA); *2xMYB-Sp*, (CGC GTCAGATTT**ATA**GGGA G**GG**GGACAGATTT**ATA**GGGAG**GG**GGAA) and (GATCTTCC**CC** CTCCC**TAT**AAATCTGTCC**CC**CTCC C**TAT**AAATCTGA); and *2xMYB-Null* (CGCGTCAGAT TT**ATA**GGGAG**AT**GGACAGATTT**ATA**GGGA G**AT**GGAA) and (GATCTTCC**AT**CTCCC**TAT** AAATCTGTCC**AT**CTCCC**TAT**AAATCTGA), oligonucleotides were ligated to pBG-LUC, immediately upstream from the ß-globin TATA box.

To generate *MYBpr-Luc* and its mutant derivatives, PCR products encompassing the *MYB* promoter (−687 to +5 relative to the transcription start site) were obtained from myb(WT)-Luc, myb(E2F)-Luc, myb(myb-sp)-Luc and myb(null)-Luc (5) and cloned into pGL2-Basic. PCR primer sequences were as follows (5′-3′): GACTTCGGAT CCGGGAGGGAGTGAA AGCTC and GAAGTCGG ATCCTTAAAGTGTAAACTCTGTAAACAG. To generate *MYBpr(+205)-Luc* and its mutant derivatives, the *MYB* 5′UTR was obtained from B1-CAT (19) and cloned directly downstream from the WT or mutant versions of the *MYB* promoter into *MYBpr-Luc*.

Knockdown plasmids were generated by cloning *MAZ*-specific shRNAs (*shMAZ-A* and *shMAZ-B*) or a control shRNA into the lentiviral plasmid, pLVTHM (a gift from D. Trono's lab). The shRNA sequences used (5′-3′) were as follows: *shMAZ-A*: CGCGTGGTACTGGTGA GGTTTGTCCAATGGCGGCATCTAGAGCCGCCA TTGGACAAACCTCACCAGTACCTTTTTTAT and CGATAAAAAAGGTACTGGTGAGGTTTGTCCAA TGGC GGCTCTAGATGCCGCCATTGGACAAA CCTCACCAGTACCA; *shMAZ-B*: CGCGTCCCTCA ACAGTCACGTCAGACAAGTGCAATCTAGAT GCACTTGTCTGACGTGACTGTTGAGGTGTT TTTTAT and CGATAAAAAACACCTCAACA GTCACGTCAGACAAGTGCATCTAGATTGCA CTTGTCTGACGTGACTGTTGAGGTGA; Control: CGCGTTTAATATCAAGGGACACAATC AGTATTACATCTAGAGTAATACTGCTTGTGTC CCTTGATATTAATTTTTTAT and CGATAA AAAA TTAATATCAAGGGACACAATCAGTATTACTCT AGATGTAATACTGCTTGTGTCCCTTGATATTAAA. All plasmids were sequence verified.

Chromatin immunoprecipitation (ChIP)

Chromatin immunoprecipitation (ChIP) was done as described (16) with modifications to enable lymphocytes chromatin fragmentation. Briefly, cells were treated with 1% formaldehyde for 10 min at RT and subsequently with 1.25 M glycine for 5 min. Nuclei were frozen at −80°C before treating them with 0.15 u micrococcal nuclease (8805, Thermo Scientific) for 5 min at 37°C. Reaction was stopped with 1% SDS plus 5 mM Ethylene glycol-bis(2-aminoethylether)-N,N,N′,N′-tetraacetic acid (EGTA). Digested chromatin was sonicated (8 pulses of 30 s) in a sonicator bath and cell debris was eliminated by centrifugation (15 min, 17 000 × *g*, 4°C). The average DNA length achieved was 200–600 bp. Fragmented chromatin was pre-cleared with protein A-Sepharose beads (preincubated with sonicated salmon sperm DNA, BSA and normal rabbit serum) and immunoprecipitated with Rabbit anti-mouse IgG (M7023, Sigma), anti-MAZ M-123 or anti-RNA Polymerase II (MMS-126R; Covance). Immunoprecipitated complexes were collected with Protein A-Sepharose beads pre-incubated with sonicated salmon sperm DNA and BSA. The beads were washed and eluted, and DNA was extracted from the eluates according to the ChIP Assay Kit protocol (Upstate). One-third of the final volume was analyzed by Syber-Green real time PCR using the following oligonucleotides:

DNA was analyzed by Sybr Green real-time PCR using specific primers that amplified the *MYB* promoter, the *POLR2A* promoter or the 5′-UTR of *BMP7*: Mybchip1-F (GAGCGGGGTTTGCTCAGGAAAAGGC), Mybchip1-R (AAGAGCTTTGGACACTCCCCCT CCC), Pol2-F (GAGAAGAAGGCGGCTCCCG-GAAGG) Pol2-R (CCGCCTAGGTGCTCAG AC-CTCGTCAG), Bmp7-F (GGCTTCTCCTACCCCTA-

CAAGGCCGT), Bmp7-R (CGGAGGAT CCCTCCTTC-CCAGTAACC).

Transfections and reporter gene assays

Saos-2 and HEK-293T cells were transfected by employing the calcium phosphate method (20). Transfections of Saos-2 cells included 10 μg of appropriate firefly luciferase reporter plasmid plus 0.1 μg of pRL-Null (Promega, Madison, WI, USA) and 20 μg of carrier plasmid (Bluescript; Stratagene, Agilent Technologies, Santa Clara, CA, USA). Where indicated, pRc-CMV-E2F1 plus pRc-CMV-DP1, pcDNA3-HA-RB, pcDNA3-HA-p130 and/or increasing amounts of pcDNA3-HA-MAZ1, -MAZ2 or -MAZ-2s were also used. In control transfections, mock pcDNA3 or pRc-CMV was used. PBLs were harvested and resuspended at a density of 1×10^8 cells/ml in RPMI 1640 and, then, electroporated as described previously (21). Transfected PBLs were split in two 35-mm-diameter dishes, incubated in RPMI with 10% FCS at 37°C and activated or not with 5 μg/ml leucoagglutinin (Sigma–Aldrich) plus 50 U/ml IL-2 for 24 h. PBLs transfection included 40 μg *MYBpr(+205)-Luc* reporter vectors and 5 μg pRL-SV40 (Promega Biotech, Madrid, Spain). Firefly and Renilla luciferase activities were assayed using Dual Luciferase Reporter Assay System (Promega). Firefly luciferase activity was normalized with that of Renilla luciferase.

Lentiviral production and infection

Lentivirus expressing green fluorescent protein (GFP) and MAZ-specific shRNAs or scrambled shRNA sequences were obtained, as previously described (22), by transient calcium-phosphate transfection of HEK-293T cells, using pLVTHM, psPAX2 and pMD2G-VSVG plasmids provided by D. Trono (Ecole Polytechnique Federale de Lausanne, Lausanne, Swisse). The supernatant containing the lentiviral particles was collected 48 h after removal of the calcium phosphate precipitate, filtered through a 45-μM polyvinylidene difluoride (PVDF) membrane (Steriflip; Millipore), concentrated by ultracentrifugation (88 000 × *g*, 2 h at 4°C) and stored at −80°C. Functional viruses were titrated by infecting Jurkat cells with limiting virus dilutions and quantification of GFP positive cells by flow cytometry after 24 h. Similar infection efficiencies with the different constructs were found across experiments. IL2-dependent, proliferating lymphocytes (10^7 cells) were infected 10 days after leucoagglutinin stimulation by adding lentivirus particles (MOI = 50) and incubating for 48 h. At this time, blast cells were ≥98% positive for CD3 expression (a marker of T lymphocytes) as determined by flow cytometry analysis. Cells were subsequently washed with RPMI 1640 medium and transferred to culture medium without IL2. Two days later, cells were stimulated again with 5 μg/ml leucoagglutinin plus 50 U/ml of IL2 or left untreated. Infection efficiency (GFP expression) was monitored by flow cytometry.

Quantitative PCR analysis

Total RNA was extracted from 5×10^6 lymphocytes using RNeasy (74104; Qiagen, Venlo, Netherlands). The genomic facility at Instituto de Investigaciones Biomedicas synthesized complementary DNA using M-MLV retro transcriptase (ThermoFischer Scientific) and analyzed gene expression by real-time quantitative (RT-qPCR) as described (23) using TaqMan Gene Expression Assays (ThermoFischer Scientific) specific for human *MAZ* (Hs00911157_g1), *MYB* (Hs00193527_m1), *CYCNG2* (Hs00171119_m1), *E2F1* (Hs00153451_m1) and *GUSB* (Hs99999908_m1). *GUSB* was chosen as a control gene on the basis of its homogeneous expression in stimulated and untreated lymphocytes. Each gene expression experiment was performed at least three times and calculations were made from measurements of three replicates of each sample.

Immunofluorescence

Primary lymphocytes cultured on poly-Lys-coated coverslips were fixed with 4% paraformaldehyde (PFA), permeabilized with 0.1% Triton X-100 in phosphate-buffered saline (PBS) for 5 min and then incubated in 4% BSA in PBS for 30 min. Coverslips were then incubated for 1 h at room temperature with anti-CD45 D3/9 (a generous gift of Dr F. Sanchez-Madrid) and anti-phospho-MAZ (S460) in blocking solution followed by the corresponding secondary antibody. The nuclei were stained with DAPI and coverslips were mounted with Prolong medium (ThermoFisher Scientific, Waltham, MA, USA). Confocal microscopy images were acquired using plan-apochromatic objectives in an inverted Zeiss LSM 710 laser-scanning microscope (Zeiss, Germany). Sequential scanning mode was used to avoid crosstalk between channels. All images shown correspond to single sections. Pictures were processed with Zen 2009 (Carl Zeiss MicroImaging) and Adobe Photoshop CS (Adobe Systems Inc.) software.

Statistical analysis

Experiments were performed at least three times. Graphpad Prism software 6.01 was used for the analysis. Differences were analyzed by one-way or two-way analysis of variance (ANOVA) with Bonferroni post-tests, as appropriate. Differences were considered significant at $P < 0.05$.

RESULTS

Myb-sp contains a 30 kDa DNA-binding protein

EMSA of nuclear extracts from the B-cell line DG-75 and the E2F element in the *MYB* promoter (*MYB*-E2F) showed, as previously described with other cells (5), four major protein complexes (I–IV) that are common to other E2F probes (Figure 1A). In addition, the *MYB*-E2F site formed an additional complex (complex V) that was not observed with any of the other E2F elements (Figure 1A). While complexes I to IV contained E2F/DP heterodimers associated to p107 (complex I), RB (complex II) or to no RB family member (complexes III and IV), complex V contained no DP/E2F factors (5). Given the specificity of complex V, its constituent nuclear factor was named Myb-sp (5).

Since Myb-sp did not contain any DP/E2F factor, we hypothesized that, by using UV cross-linking, we might uncover a protein component of complex V that would not be

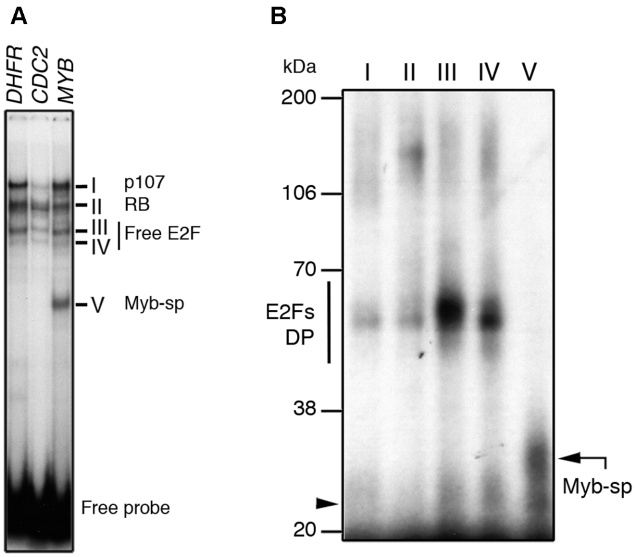

Figure 1. Identification of a 30-kDa DNA-binding protein in Myb-sp. (**A**) Complex formation employing nuclear extracts from the lymphoma B-cell line DG-75 and radiolabeled E2F elements from the *DHFR*, *CDC2* and *MYB* promoters were analyzed by EMSA. The position of complexes I–V, containing p107, RB, free E2F or Myb-sp is indicated. The free *MYB-E2F* probe is indicated. (**B**) Relative molecular weight estimation of DNA-binding components of complexes formed with the *MYB-E2F* probe. Ultraviolet (UV) cross-linking analysis of complexes I–V was performed employing DG-75 nuclear extracts and a bromodeoxyuridine-substituted *MYB-E2F* probe. Following native gel electrophoresis, the gel was irradiated with UV light and the indicated complexes were excised from the gel. Labeled proteins in the excised bands were then separated by electrophoresis in a 10% SDS-PAGE. The gel mobility of pre-stained protein molecular weight markers following compensation for the size of the cross-linked probes (11 kDa) is indicated in kDa. The arrow indicates the position of Myb-sp.

present in complexes I–IV. UV cross-linking of complexes I–IV revealed strong and specific bands of 45–60 kDa (Figure 1B), which are consistent with the expected size of DP and E2F subunits and with previous results using other *E2F* elements or cells (13). In contrast, the only specific band observed upon UV cross-linking of Myb-sp (complex V) showed an apparent mass of 30 kDa (Figure 1B).

Myb-sp contains the transcription factor MYC-associated zinc finger protein (MAZ)

To identify the 30-kDa-protein present in Myb-sp, we purified this factor by affinity chromatography. We had previously identified the key nucleotides of the *MYB*-E2F site required for binding of either E2F factors or Myb-sp (5) and used this information to design oligonucleotides that bind only Myb-sp (*MYB-Sp*), only E2F (*MYB-E2F*) or no factor (*MYB-Null*) (Figure 2A). As expected, complex formation employing DG-75 nuclear extracts and the wild-type (WT) probe (*MYB-WT*) was competed with a self-oligonucleotide, but not with the *Null* mutant (Figure 2B). Notably, the *MYB-Sp* oligonucleotide inhibited formation of complex V, but did not affect complexes I-IV (Figure 2B). In contrast, the *MYB-E2F* oligonucleotide inhibited complexes I-IV, but did not affect complex V appearance (Figure 2B).

DNA affinity columns were then prepared by covalently binding concatemerized *MYB-Sp* or *MYB-Null* oligonucleotides to sepharose beads. Nuclear extracts from DG-75 cells were loaded onto both affinity columns and proteins bound to the beads were eluted with an excess of *Sp* oligonucleotides and fractionated through SDS-PAGE. The presence of a silver-stained band of 30 kDa (B30) was detected only in the proteins eluted from the *Sp* column (Figure 2C). Mass spectrometry analysis of tryptic peptides derived from this band detected seven peptides that were unequivocally identified as peptides from the MAZ family of zinc finger proteins (Figure 2D and Supplementary Figure S1).

MAZ is expressed in humans as three major isoforms, MAZ-1 (477 aa), MAZ-2 (493 aa) and MAZ-3 (454 aa) (Figure 2E and Supplementary Figure S1) (24–26). A shorter MAZ-2 protein, encompassing only aa 229–493 (hereafter referred to as MAZ-2s) has also been found (27). MAZ-1 and MAZ-2 share 427 aa and differ only in their carboxy-terminal tails, whereas the first 34 aa of MAZ-1 have been substituted in MAZ-3 by a sequence of 13 aa that is not present in MAZ-1 or MAZ-2 (Figure 2E and Supplementary Figure S1B). All isoforms contain a DNA-binding domain, a nuclear localization signal, and several domains that positively or negatively regulate transcription (Supplementary Figure S2), as described for MAZ-1 (28).

While six of the seven tryptic peptides identified in band B30 were common to all MAZ isoforms, one peptide was found only in MAZ-2 or MAZ-2s (Figure 2D and Supplementary Figure S1), strongly suggesting that MAZ-2 and/or MAZ2-s are present in Myb-sp. Since the theoretical mass of MAZ-2 (51 073 Da) is much larger than that of the purified protein or that of the DNA-binding protein detected by UV cross-linking, we hypothesized that the MAZ-2 isoform present in Myb-sp might be MAZ-2s (theoretical mass of 28 621 Da).

To determine whether MAZ-2s is the only MAZ protein in Myb-sp or if other MAZ family members might also be present in this complex, we first tested the ability of *in vitro* translated (IVT) MAZ-2s and MAZ-1 to bind the *MYB*-E2F site in EMSA assays. As expected five major complexes were observed employing a nuclear extract from DG-75 cells (Figure 2F). A major complex, showing a similar mobility to that of Myb-sp, was detected employing IVT MAZ-2s or MAZ-1 (Figure 2F). Formation of this complex was efficiently competed by a self-oligonucleotide and by its mutant derivative *Sp*, but not by its *E2F* or *Null* mutant derivatives (Figure 2F). These results strongly suggest that all MAZ proteins are capable of binding the *MYB*-E2F site. Only one major complex, with a similar mobility to that of complex III, was observed employing a control reticulocyte lysate (Figure 2F). This complex appeared to be specific and might perhaps contain E2F from the reticulocytes because its formation was efficiently competed by a self-oligonucleotide and by its mutant derivative that binds only E2F factors, but not by its mutant derivatives *Sp* or *Null* (Figure 2F).

To further confirm that Myb-sp contains MAZ factors, we generated antibodies against different MAZ isoforms and used them as competitors in EMSA assays to identify the isoforms involved in complex formation. Peptides from the amino- or carboxy-terminal end of MAZ-1, MAZ-

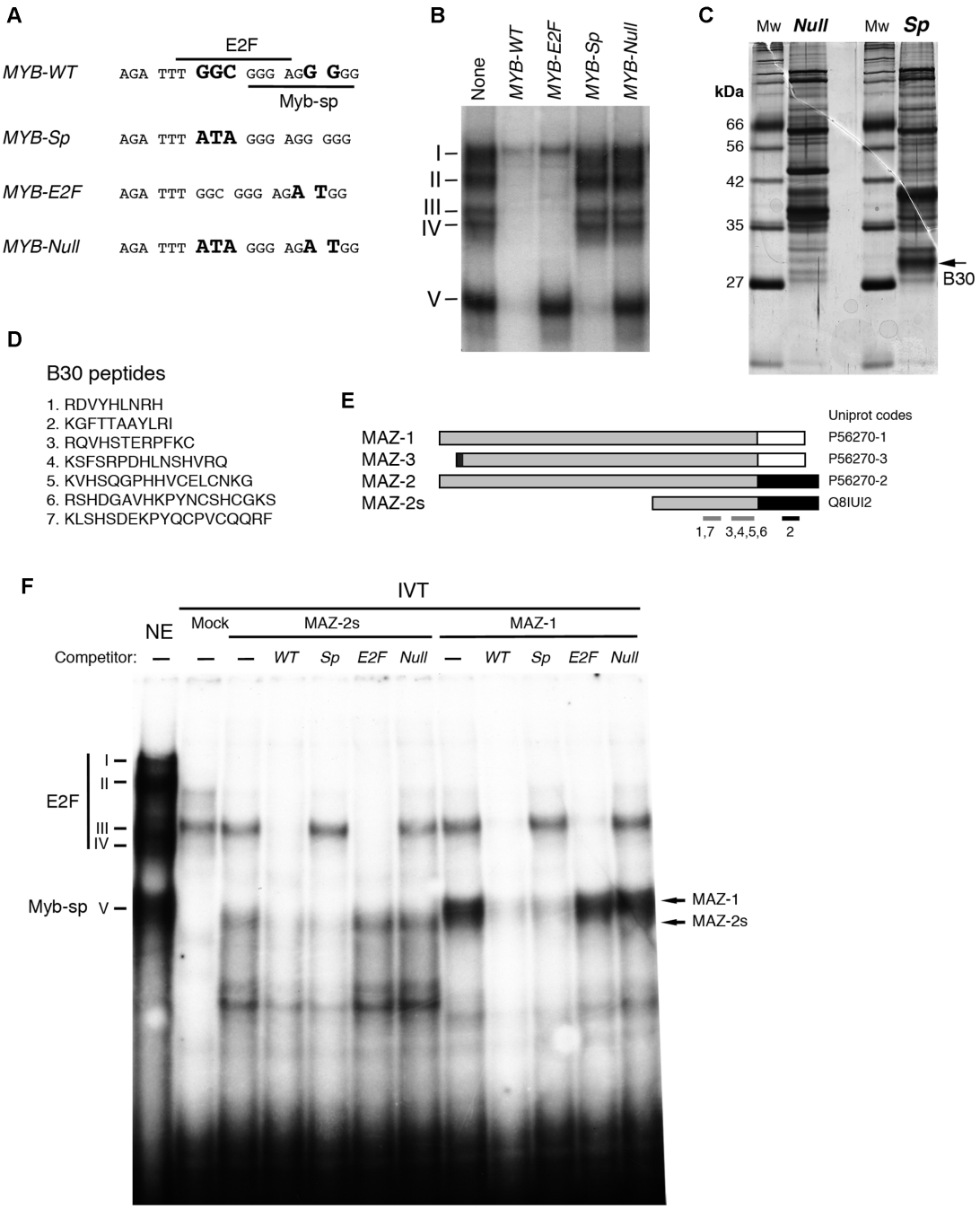

Figure 2. Myb-sp contains the transcription factor MAZ. (**A**) Sequence of WT and mutant *MYB-E2F* probes. For each mutant, alterations relative to the WT sequence are indicated in bold. Lines indicate the binding sites for E2F and Myb-sp. (**B**) Complexes formed between DG-75 nuclear factors and the radiolabeled *MYB-E2F* probe were analyzed by EMSA. Reaction mixtures were incubated in the absence (indicated as None) or in the presence of a 100-fold excess of the indicated unlabeled competitor oligonucleotides. The position of complexes I–V is denoted. The free probe is not shown. (**C**) A nuclear extract derived from DG-75 cells was subjected to sequence-specific DNA affinity chromatography employing concatemerized *MYB-Sp* or *MYB-Null* oligonucleotides bound to sepharose beads. Samples were eluted with an excess of *MYB-Sp* oligonucleotides and analyzed by 10% SDS-PAGE and silver staining. A 30-kDa band (B30) was excised and subjected to mass spectrometry analysis. (**D**) Sequence of the seven tryptic peptides derived from B30. (**E**) Schematic representation of major MAZ isoforms. The Uniprot code of these isoforms and the approximate position of the detected peptides are indicated. (**F**) EMSA analysis of complex formation employing the radiolabeled *MYB-E2F* probe and a nuclear extract from DG-75 cells (NE), a control reticulocyte lysate (Mock) or *in vitro* translated MAZ-2s or MAZ-1. Reaction mixtures were incubated in the absence or in the presence of a 100-fold excess of the indicated unlabeled *MYB-E2F* competitor oligonucleotides.

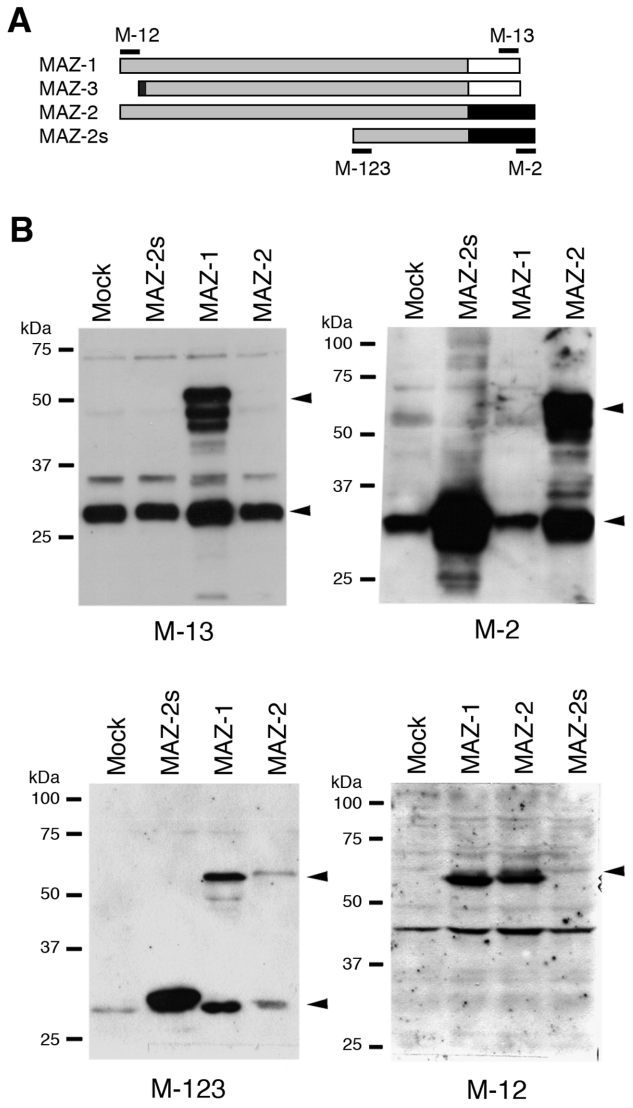

Figure 3. Production of antibodies against various MAZ isoforms. (**A**) Schematic representation of major MAZ isoforms indicating the approximate position of the peptides employed as immunogens in the production of the indicated anti-MAZ antibodies. (**B**) Immunoblot analysis employing the indicated anti-MAZ antibodies and protein extracts derived from HEK-293T overexpressing MAZ1, MAZ-2, MAZ-2s or from Mock-transfected cells. Arrowheads indicate the position of the major proteins identified by these antibodies.

2 or MAZ-2s were used as immunogens to generate polyclonal rabbit antibodies (Figure 3A). The specificity of these antibodies was confirmed by immunoblot of cell lysates from HEK-293T cells forced to express MAZ-1, MAZ-2 or MAZ-2s. The M-13 antibody, raised against a peptide from the carboxy-terminal end of MAZ-1 and MAZ-3 (Figure 3A), specifically recognized ectopically expressed MAZ-1 and a major endogenous protein of ∼30 kDa (Figure 3B). The M-2 antibody, raised against a peptide from the carboxyl-terminal end of MAZ-2 (Figure 3A), detected ectopically expressed MAZ-2 and MAZ-2s and a major endogenous protein of ∼30 kDa (Figure 3B). The M-123 antibody, raised against a peptide from the amino-terminal end of MAZ-2s (common to all isoforms; Figure 3A), recognized ectopically expressed MAZ-1, MAZ-2 and MAZ-2s (Figure 3B). Of note, this antibody also hybridized strongly with an ∼30-kDa-band in cell lysates from cells forced to express full-length MAZ-1, suggesting the possibility that these cells might express high levels of a smaller version of MAZ-1 (MAZ-1s), similar to MAZ-2s. Finally, the M-12 antibody, raised against a peptide from the amino-terminal end of MAZ-1 (identical to MAZ-2; Figure 3A), recognized ectopically expressed MAZ-1 and MAZ-2, but not MAZ-2s or any other endogenous protein with a relative mass close to 30 kDa (Figure 3B).

Complex formation between the *MYB*-E2F probe and IVT MAZ-2s tagged with HA was markedly affected by an anti-HA antibody and by anti-MAZ antibodies M-2 and M-123 (Figure 4A). In contrast, the anti-MAZ M-12 and M-13, the M-123 pre-immune serum or an antibody to Smad2/3 failed to shift the mobility of the complex (Figure 4A). A similar complex was observed employing IVT MAZ-1 (Figure 4A) and its formation was inhibited by anti-MAZ M-13 and M-123 antibodies, but not by anti-MAZ M-2 or anti-Smad2/3 antibodies or by pre-immune sera (Figure 4A). The M-12 antibody also failed to affect the formation of this complex (Figure 4A), suggesting that it does not work properly in EMSA assays. Together, these data indicate that MAZ-1 and MAZ-2s are able to interact with the *MYB*-E2F probe.

To determine if endogenous MAZ proteins are present in Myb-sp, we used these anti-MAZ antibodies and the *MYB*-E2F probe with nuclear extracts from DG-75 cells. M-13 and M-2 antibodies inhibited formation of the slower- and the faster-migrating portion of complex V, respectively, and the combination of both antibodies completely eliminated complex V (Figure 4B). Formation of this complex was ablated also by the M-123 antibody (Figure 4B). As expected, the formation of E2F-containing complexes (I–IV) was inhibited by an anti-DP1 antibody, but not by any of the anti-MAZ antibodies or their pre-immune sera (Figure 4B). The M-12 and anti-HA antibodies and any of the MAZ pre-immune sera failed to interfere with the formation of any of these complexes (Figure 4B). These results indicate that endogenous MAZ proteins are components of Myb-sp.

MAZ binding to the *MYB*-E2F site overcomes its repression by RB family members and activates the *MYB* promoter

As we had suggested that binding of Myb-sp to the *MYB*-E2F site prevented *MYB* promoter repression by RB family members (5), we now investigated whether MAZ factors, as Myb-sp components, might overcome transcriptional repression by pRB or p130. RB-deficient Saos-2 cells were transfected with luciferase reporter plasmids (*2xMYB-BG-LUC*) containing a *TATA* box and two copies of the wild-type (*WT*) *MYB*-E2F site (Figure 5A). We also employed previously reported (5) mutant derivatives of this site that bind only E2F, only Myb-sp (*Sp*) or no factor (*Null*). Forced expression of MAZ-1, MAZ-2 and MAZ-2s transactivated the *WT* and *Sp* reporter, but not the *E2F* or the *Null* derivatives (Figure 5B). In contrast, forced expression of E2F1/DP1 transactivated the *E2F* reporter, but not the S*p* mutant (Figure 5B). Forced pRB or p130 expression

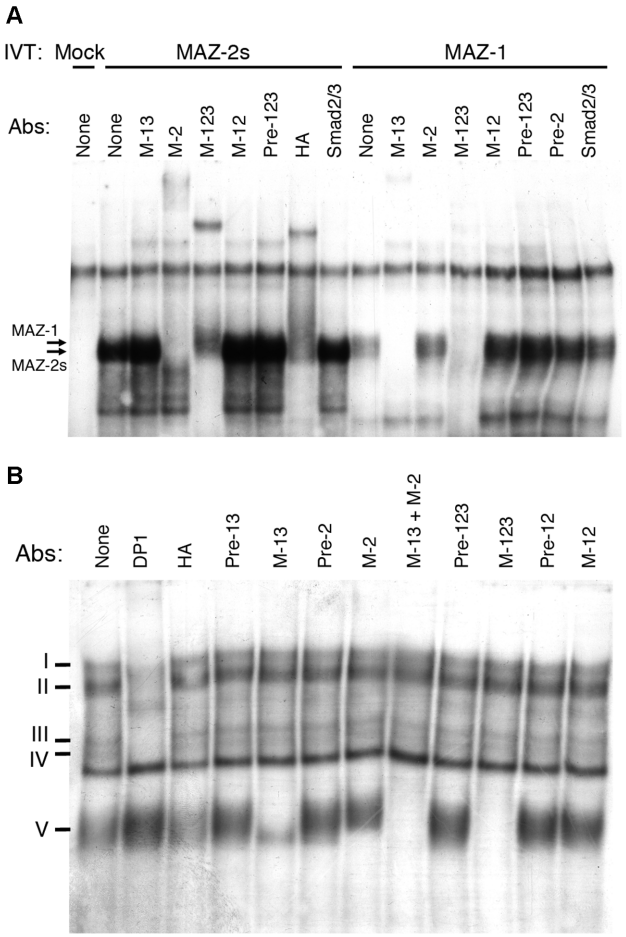

Figure 4. Myb-sp contains various MAZ isoforms. (**A**) EMSA analysis of complex formation employing the radiolabeled *MYB-E2F* probe and a control reticulocyte lysate (Mock), or *in vitro* translated MAZ-2s or MAZ-1. Reaction mixtures were incubated in the absence (none) or in the presence of the indicated anti-MAZ antibodies, the M-123 pre-immune serum (Pre-123) and an anti-HA or an anti-Smad2/3 antibody. The free probe is not shown. (**B**) EMSA analysis of complex formation employing the radiolabeled *MYB-E2F* probe and nuclear extracts from DG-75 cells. Reaction mixtures were incubated in the absence (none) or in the presence of the indicated anti-MAZ antibodies; the M-13, M-123 and M-12 pre-immune sera (Pre-13, Pre-123 and Pre-12, respectively); and an anti-HA or an anti-DP1 antibody. The free probe is not shown.

markedly reduced the activity of the *WT* and *E2F* reporters, but not that of the construct driven only by the *Sp* derivative (Figure 5C–E). Finally, RB- and p130-mediated repression of the *WT* reporter, but not that of the *E2F* derivative, was overcome by progressively increasing amounts of either MAZ-2s or MAZ-1 (Figure 5C–E). Since MAZ-2s activated transcription more poorly than MAZ-1 or MAZ-2, we compared their levels in cells transfected with plasmids encoding these isoforms together with *WT* and *Sp* reporter vectors. While all MAZ isoforms were expressed at similar levels, MAZ-2s showed less activation capacity than MAZ-1 or MAZ-2 (Supplementary Figure S3).

To assess the regulation of *MYB* transcription by MAZ factors on the complete human *MYB* promoter, we used a reporter (*MYBpr*) in which luciferase expression was under the control of the human *MYB* promoter (Figure 6A) or derivatives in which its *E2F* site was mutated to bind only E2F, only MAZ proteins (*Sp*) or no factor (*Null*), as previously described (5). Saos-2 cells were cotransfected with these reporter constructs and progressively increasing amounts of MAZ-1 or MAZ-2s expression vectors. Analysis of the luciferase activity in extracts from these cells showed that MAZ-1 and MAZ-2s activated the *WT* and the *Sp* versions of the *MYB* promoter, but not its *E2F* or *Null* mutant derivatives (Figure 6B-C). Together, these results suggest that MAZ specifically regulates the *MYB* promoter *in vivo* via the *MYB*-E2F site (*E2F/MAZ* element).

Endogenous MAZ factors bind and activate the *MYB* promoter *in vivo* and induce *MYB* expression

To determine whether MAZ regulates *MYB* expression not only in tumor cell lines, but also in healthy primary cells, we assessed its contribution to the regulation of the *MYB* promoter in primary PBLs. *MYB* is not expressed in quiescent lymphocytes but its transcription is activated early during the exit from quiescence and remains active thereafter (11,12). Since a previous report had shown inhibition of *MYB* promoter activity in HEK-293 cells by MAZ through a *GC* box in the 5′UTR of *MYB* (29), we engineered an additional reporter vector, *MYBpr(+205)*, extending the *MYB* promoter with its 5′UTR that includes the *GC* box (Figure 7A). The transfection efficiency of primary quiescent lymphocytes is extremely low, but under certain conditions it is sufficient to detect the activity of given luciferase reporters (13). The *WT* and mutant derivative *MYBpr*(*+205*) plasmids whose *E2F/MAZ* element could interact only with E2F, only with MAZ (*Sp*) or with no factor (*Null*) were transfected in quiescent PBLs. Cells were then left untreated or activated for 24 h with leucoagglutinin plus interleukin-2 (IL2) to exit from quiescence. The luciferase activity from resting and stimulated cells was measured to assess the respective transactivation capacity of each factor following lymphocyte activation. As shown in Figure 7B, the reporter plasmids that contained a WT *E2F/MAZ* site or its *Sp* mutant derivative were activated 3- to 4-fold following cell stimulation, whereas reporter plasmids that contained its *E2F* or *Null* derivatives were not activated, thus supporting the notion that MAZ binding to the *E2F/MAZ* site is required for transcriptional induction of *MYB*.

To determine whether MAZ was associated *in vivo* with the human *MYB* promoter, ChIP assays were performed with anti-MAZ M-123. Transcriptional activation of this locus 2 h after the exit from quiescence was also assessed by ChIP analysis of RNA Polymerase II (Pol II) binding to the *MYB* locus. The products of PCR reactions performed with DNA eluted from the immunoprecipitates were analyzed by RT-qPCR. ChIP assays confirmed recruitment of both MAZ and Pol II to a *MYB* promoter region encompassing the E2F/MAZ site and the transcription initiation site in cells activated in 2 h, but not in quiescent cells (Figure 7C). According to the constitutive transcription of the gene encoding Pol II (*POLR2A*), ChIP analysis showed Pol II binding in quiescent and activated cells to its own promoter (Figure 7C). In contrast, MAZ was not bound to this promoter in any condition (Figure 7C). Importantly, negative control

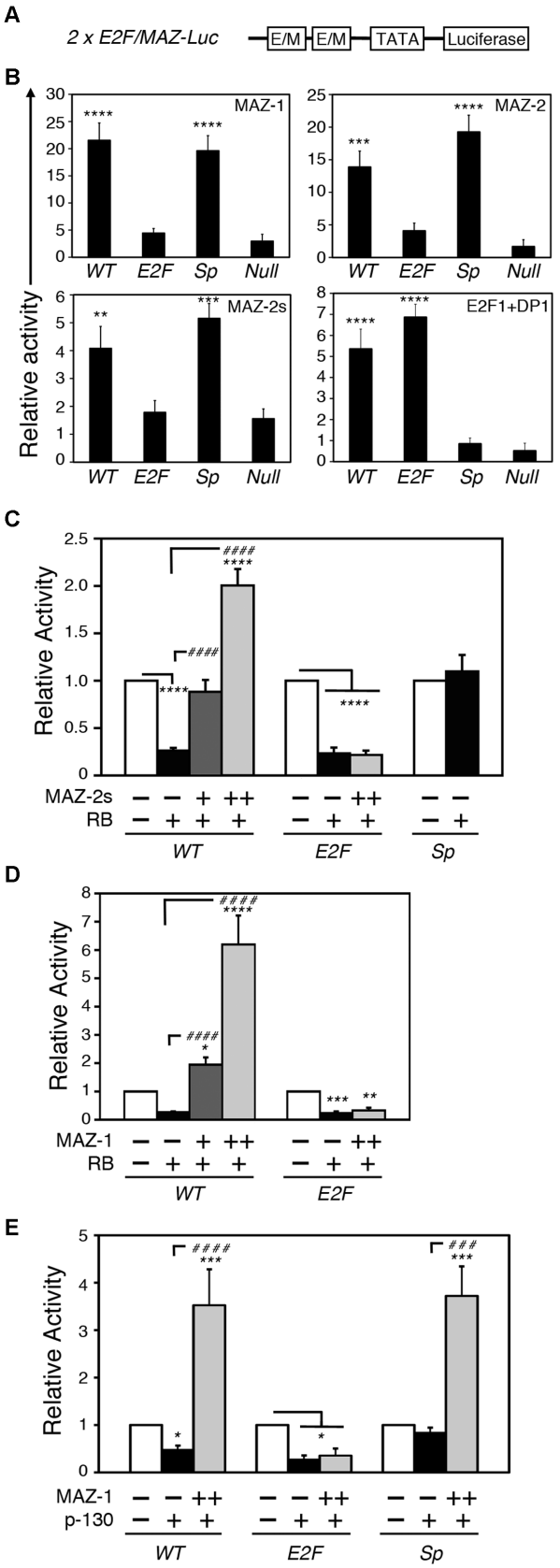

Figure 5. MAZ proteins bind the *MYB*-E2F element *in vivo* and overcome RB-mediated transcriptional repression through this element. ChIP assays using the M-123 pre-immune serum (Ctl) on these two promoters and using the anti-MAZ and anti-Pol II antibodies on the 3′-UTR of *BMP7* excluded the possibility of co-precipitation of non-specific DNA sequences (Figure 7C). These results therefore show that MAZ and Pol II bind the *MYB* promoter *in vivo* 2h after the exit from quiescence.

Since promoters cloned into reporter vectors might not necessarily be regulated as in their chromosomal context, we sought to determine the contribution of endogenous MAZ proteins to the activation of the *MYB* gene. To this end, we downregulated MAZ levels in primary cells through lentivirus-mediated expression of *MAZ* shRNAs. A screen of several *MAZ* shRNAs in the T-cell line Jurkat identified the high silencing capacity of *shMAZ-A* and *shMAZ-B* on MAZ isoforms (Supplementary Figure S6). Because lentiviral transduction of resting primary T lymphocytes is poorly efficient, we stimulated their proliferation with leucoagglutinin and IL2 before infecting them. As previously described (15), IL2 starvation of activated T lymphocytes leads them back into a quiescent state, that can be readily reverted through the addition of fresh stimuli (Figure 8A). To confirm the quiescence of these cells, we assessed the expression levels of *CCNG2* mRNA and p130, both markers of G0 whose expression decreases during the exit from quiescence (9,30,31). We found that while their expression was high in IL2-starved cells, it decreased markedly in stimulated lymphocytes (Figure 8B and Supplementary Figure S4). In contrast, the levels of *E2F1* mRNA, a gene that is not expressed in quiescent lymphocytes and that is induced at the G1-S transition (32), were low in starved cells and increased 16 h after lymphocyte stimulation (Figure 8C).

Under these conditions, *MYB* expression increased as early as 1 h after T-cell re-stimulation (Figure 8B). However, RB family members inactivation, as determined by phosphorylation of p130 and pRB, was not observed before 8 h from quiescence exit (Figure 8B). MAZ protein in the nucleus and its mRNA levels were not substantially af-

(**A**) Schematic representation of the luciferase reporter plasmids used, *2xE2F/MAZ-Luc*. Two copies of the WT E2F site from the *MYB* promoter or its mutant derivatives that interact only with E2F (*E2F*), only with MAZ (*Sp*) or with none of them (*Null*) were cloned immediately upstream from the *ß-globin TATA* box in *pBG-Luc*. (**B**) The indicated *2xE2F/MAZ-Luc* plasmids (1 μg) were cotransfected with *pRL-null* (1 μg) in asynchronously growing Saos-2 cells in the presence of plasmids encoding MAZ-1 (0.1 μg), MAZ-2 (0.1 μg), MAZ-2s (0.1 μg), DP1 (50 ng) plus E2F1 (50 ng) or empty vector (0.1 μg). Forty hours later, cell extracts were prepared and firefly and renilla luciferase assays were performed. Firefly luciferase values were normalized for renilla activity. Luciferase activity is shown relative to that in the presence of the empty vector (mean ± SEM; $n = 4$). $^{**}P < 0.01$, $^{***}P < 0.001$ and $^{****}P < 0.0001$ versus *Null*; one-way ANOVA with Bonferroni post-test. (**C**–**E**) The indicated *2xE2F/MAZ-Luc* (1 μg) plasmids were cotransfected with *pRL-null* (1 μg) in asynchronously growing Saos-2 cells in the presence of 0.1 μg of empty vector (−), or plasmids encoding either (C and D) pRB (0.1 μg) or (E) p130, together with (C) MAZ-2s (0.1 or 0.5 μg), (D) MAZ-1 (0.1 or 0.5 μg) or MAZ-1 (0.5 μg), as indicated. Forty hours later, cell extracts were prepared and firefly and renilla luciferase assays were performed. Firefly luciferase values were normalized for renilla activity. Luciferase activity is shown relative to that in the presence of the empty vector (mean ± SEM; $n = 5$). (C and D) $^{*}P < 0.05$ and $^{****}P < 0.0001$ versus empty; $^{\#\#\#\#}P < 0.0001$ versus RB; one-way ANOVA with Bonferroni post-test.

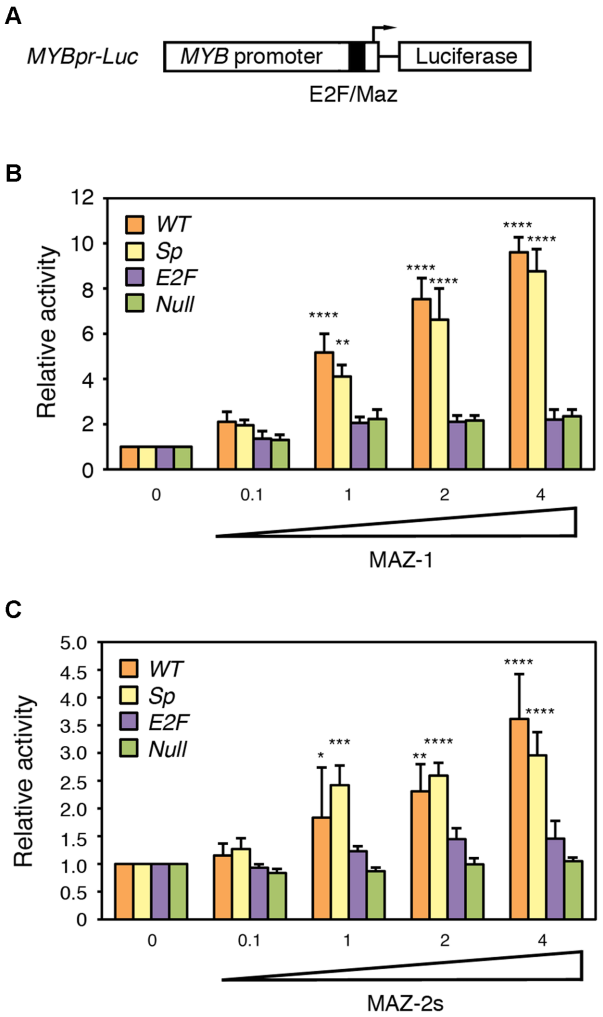

Figure 6. MAZ proteins activate the *MYB* promoter through the E2F/MAZ-binding element. (**A**) Schematic representation of the luciferase reporter vector driven by the *MYB* promoter (*MYBpr-Luc*). The position of the *E2F/MAZ* combined element (black box) and that of the transcription initiation site (arrow) is indicated. Reporter vectors with a WT *E2F/MAZ* element (*WT*) as well as vectors with a mutated site that interacted only with E2F (*E2F*), only with MAZ (*Sp*) or with none of them (*Null*) were also generated. (**B** and **C**) The indicated *MYBpr-Luc* reporter plasmids (10 μg) were cotransfected with *pRL-null* (1 μg) into Saos-2 cells in the presence of empty vector (0) or increasing amount of plasmids (indicated in μg) encoding (B) MAZ-1 ($n = 4$) or (C) MAZ-2s ($n = 3$). Forty hours later, cell extracts were prepared and firefly and renilla luciferase assays were performed. Firefly luciferase values were normalized for renilla activity. Luciferase activity is shown relative to that in the presence of the empty vector (mean ± SEM). $*P < 0.05$, $**P < 0.01$, $***P < 0.001$ and $****P < 0.0001$ versus *Null*; one-way ANOVA with Bonferroni post-test.

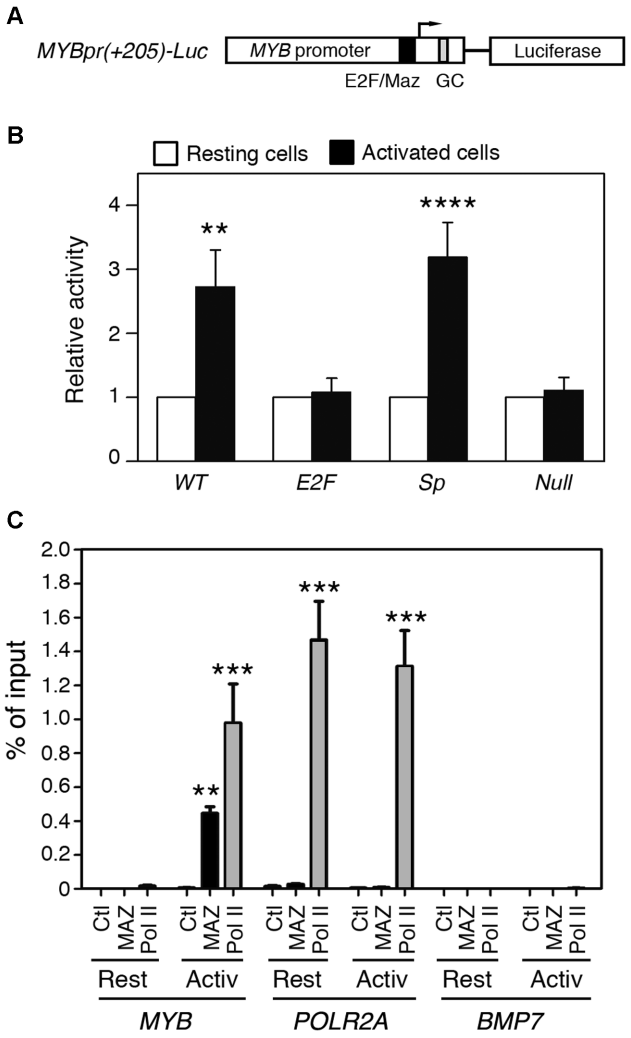

Figure 7. Activation of the *MYB* promoter during the exit from quiescence requires its MAZ-binding site. (**A**) Schematic representation of the luciferase reporter vector used, *MYBpr(+205)-Luc*. A DNA insert encompassing the *MYB* promoter plus its 5′UTR (a 205-bp DNA fragment) were cloned into *pGL2-Basic*. Reporter vectors with a WT *E2F/MAZ* element (*WT*) as well as vectors with a mutated site that interacted only with E2F (*E2F*), only with MAZ (*Sp*) or with none of them (*Null*) were also generated. The relative positions of the combined *E2F/MAZ* element (black box), the transcription initiation site (arrow) and the GC box (gray block) are shown. (**B**) The indicated *MYBpr(+205)-Luc* reporter plasmids (40 μg) were cotransfected with *pRL-SV40* (5 μg) into primary peripheral blood lymphocytes (PBLs). Following transfection, cells were split and either activated for 24 h with leucoagglutinin plus interleukin-2 to exit from quiescence (Activated cells) or left untreated (Resting cells). Firefly and renilla luciferase activities were measured in cell extracts from both activated and untreated cells. Normalized luciferase values for each indicated reporter plasmid are shown relative to untreated cells (mean ± SEM; $n = 8$). $**P < 0.01$, $****P < 0.0001$ versus *Null* Activated; two-way Anova with Bonferroni post-test. (**C**) Anti-Pol II, anti-MAZ M-123 or pre-immune M-123 (Ctl) ChIP analyses of resting lymphocytes (Res) and lymphocytes activated for 2 h (Activ). Different dilutions of input chromatin DNA (1, 0.25 and 0. 1%) or DNA extracted from the indicated immunoprecipitates were analyzed by real-time PCR using oligonucleotides flanking a *MYB* genomic region encompassing the E2F/MAZ site and the transcription initiation site (*MYB*), the transcription initiation site of *POLR2A* or the 3′-UTR of *BMP7*. Data are shown as enrichment in the amount of chromatin precipitated with each antibody relative to 0.1% input chromatin. Histograms show means ± SEM ($n = 3$). $**P < 0.01$, $***P < 0.001$ versus Ctl in quiescent cells; two-way ANOVA with Bonferroni post-test.

fected following exit from quiescence (Figure 8C and D). In contrast, the nuclear presence of an ∼50 kDa MAZ form phosphorylated at S460, a modification that enhances MAZ DNA-binding activity (33), increased markedly 1 and 3 h after quiescence exit (Figure 8D). Immunofluorescence analysis of synchronized lymphocytes confirmed augmented phospho-MAZ (S460) signal in the nucleus of cells 3h after quiescence exit relative to unstimulated cells (Supplementary Figure S5).

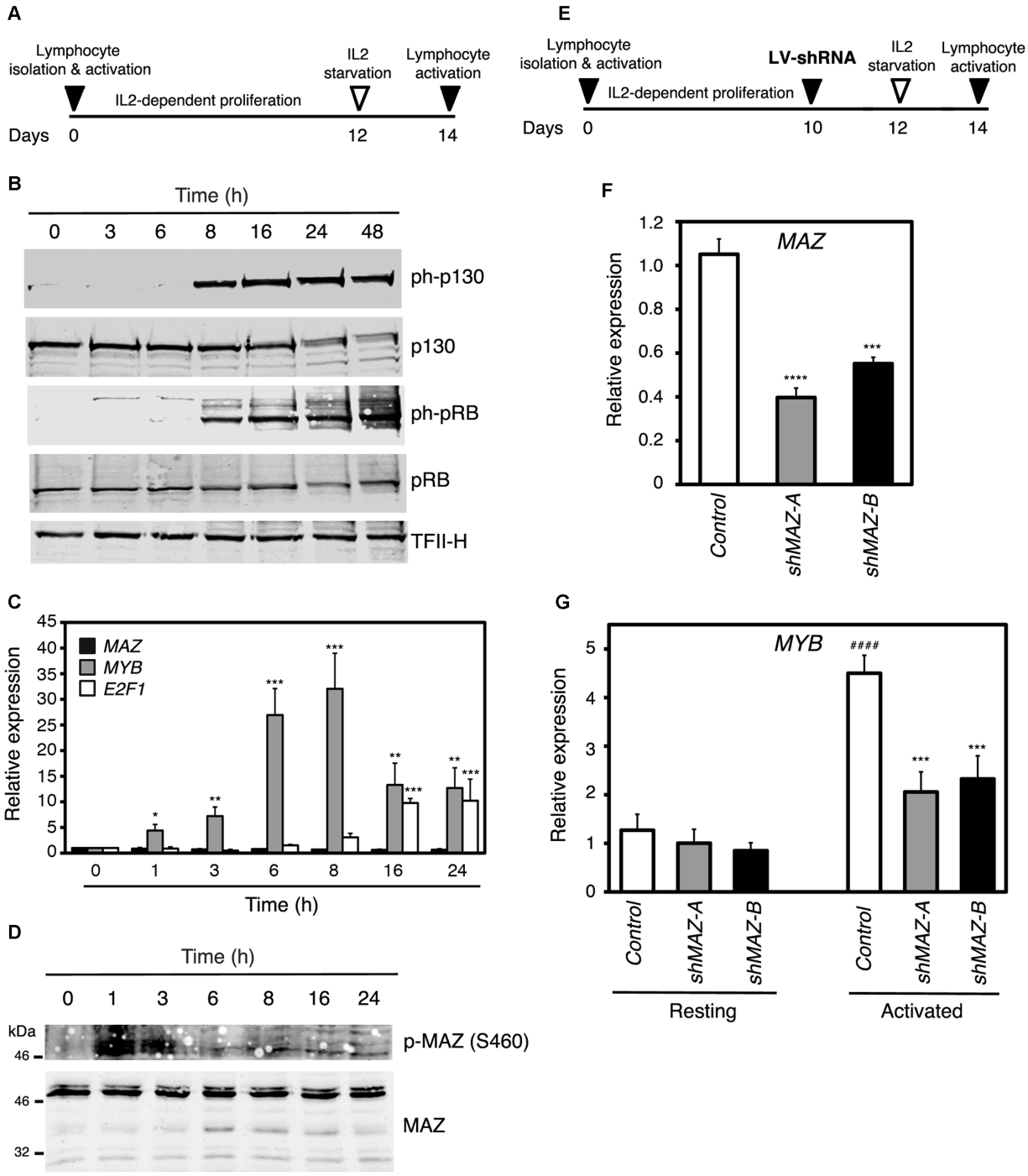

Figure 8. *MAZ* is required for *MYB* induction during the exit from quiescence. (**A**) Experimental timeline. The proliferation of isolated primary PBLs was induced with a combination of leucoagglutinin and IL2 and maintained by the presence of IL2 during 12 days. Cells were then made quiescent by IL2 starvation and induced to re-enter the cell cycle 48 h later by adding leucoagglutinin and IL2. (**B**) Immunoblot analysis of p130 phospho-S672; p130 total; a combination of pRB phospho-S780, phospho-S795 and phospho-S807/811; pRB total; and TFIIH (loading control) in nuclear extracts from these cells. (**C**) RT-qPCR analysis of *MYB, MAZ* and *E2F1* mRNA expression in lymphocytes stimulated for the indicated periods of time to re-enter the cell cycle. mRNA amounts were normalized to *GUSB* expression. Data are shown as means ± SEM ($n = 3$) relative to 0 h. $^{*}P < 0.05$, $^{**}P < 0.01$, $^{***}P < 0.001$ versus 0 h; two-way ANOVA with Bonferroni post-test. (**D**) Immunoblot analysis of phospho-MAZ (S460) and MAZ total levels (employing the MAZ-123 antibody) in nuclear extracts from these cells. (**E**) Experimental timeline as in (A). Proliferating lymphocytes were transduced with lentivirus expressing GFP and either a control shRNA or *MAZ*-specific shRNAs *sh59* or *sh60* 2 days before IL2 starvation. (**F** and **G**) Lymphocytes transduced with lentivirus expressing shRNAs as indicated were forced to become quiescent by IL2 starvation for 48 h. (E) *MAZ* knockdown was confirmed by RT-qPCR analysis at this time. mRNA amounts were normalized to *GUSB* expression (means ± SEM, $n = 3$). $^{***}P < 0.001$, $^{****}P < 0.0001$ versus *Control*; one-way ANOVA with Bonferroni post-test. (F) Transduced, quiescent cells were treated with leucoagglutinin plus IL2 for 1 h to re-enter the cell cycle (Activated) or left untreated (Resting). *MYB* mRNA levels were determined by RT-qPCR analysis and normalized to *GUSB* expression (means ± SEM, $n = 3$). $^{***}P < 0.001$ versus *Control* Activated; $^{\#\#\#\#}P < 0.0001$ versus *Control* Resting; two-way ANOVA with Bonferroni post-test.

Ten days after the activation of T lymphocytes, we transduced them with lentivirus co-expressing GFP and either *shMAZ-A* or *shMAZ-B* (Figure 8E). The transduction efficiency under these conditions varied from 50 to 70% between experiments, as determined by flow-cytometry analysis of GFP expression. These cells were IL2-starved 48 h after transduction to make them quiescent, and restimulated 2 days later to induce *MYB* expression (Figure 8E). *shMAZ-A* and *shMAZ-B* decreased *MAZ* levels 60 and 50%, respectively (Figure 8F). Of note, *MYB* induction in these cells was also markedly decreased after 1 h of stimulation relative to control cells (Figure 8G), indicating that MAZ is a critical mediator of *MYB* induction during the exit from quiescence. Together, our results strongly suggest that the E2F/MAZ element plays a crucial role during *MYB* activation in cells coming out of quiescence and that MAZ binding to this element might be critical for the early activation of *MYB* transcription.

DISCUSSION

We hypothesized that the interaction of proteins distinct from E2F with the E2F-binding site in the *MYB* promoter may prevent its transcriptional repression by E2F-recruited RB family members. Here, we have identified these proteins as members of the MAZ family of transcription factors. We have shown that MAZ proteins bind the *MYB*-E2F site *in vitro* and the *MYB* promoter *in vivo* and that they are critical not only to overcome transcriptional repression by RB family members, but also to activate transcription and that this regulation is essential for *MYB* induction during the exit from quiescence.

The regulation of *MYB* transcription is particularly complex because both its initiation and its elongation are critical. Its transcriptional initiation is regulated by several factors, including MYB itself, NF-kB, JUN, PU.1 and E2F (6,19,34–38). Indeed, forced E2F1 expression activates *MYB* transcription through its *E2F* element (6), thus indicating that this site can contribute to *MYB* promoter activation. E2F-mediated recruitment of RB family members to transcriptional regulatory regions plays a dominant negative role on gene expression (8,9). Consequently, most E2F-regulated genes are not activated before the G1-S transition, when RB family members are inactivated and released from E2F-bound promoters through their CDKs-mediated hyperphosphorylation. The *MYB* and *MYC* genes harbor E2F sites in their regulatory regions and are therefore expected to remain repressed by the E2F/p130-containing DREAM complex; both genes are activated however during the exit from quiescence (11,12,39), much earlier than the CDK-mediated inactivation of the RB family and its release from E2F factors. We have previously reported that two unidentified factors distinct from E2F, Myb-sp and EMYCS, bind respectively the *MYB* and *MYC* promoters through elements that overlap their *E2F* sites and proposed that these factors might help these genes to overcome their repression by RB family members during the exit from quiescence (5,13). EMYCS is unable to interact with the *MYB*-E2F site and shows an apparent mass of 105 kDa (13), whereas Myb-sp is unable to bind the *MYC*-E2F element and its apparent mass is 30 kDa. It thus seems that different E2F-regulated promoters are able to overcome RB family-mediated repression in G1 through the occupancy of their *E2F* sites by distinct proteins. EMYCS identity remains unknown, but we have uncovered now that Myb-sp contains MAZ proteins, also known as serum amyloid A activating factor (SAF) and Pur-1 (40,41).

The MAZ family of zinc finger proteins was first identified as a transcription factor in the *MYC* promoter (24,42). MAZ binds GC-rich sequences, namely GGGAGGG or CCCTCCC, and plays an important role in modulating TATA-less gene transcription (43–47). MAZ is expressed ubiquitously at different levels in different tissues (48) and regulates the expression of a variety of genes besides *MYC*, including *INS* (40), *CD4* (49), *SAA1* (41), *HTR2A* (45), *PNMT* (43), *FIBG* (50), *CLCNKA* (51), *RASH* (52) and *ADAM10* (53). Persistent high levels of MAZ are linked to various pathophysiological conditions, including amyloidosis, rheumatoid arthritis, atherosclerosis and the terminal phase of chronic myeloid leukemia (54–56). MAZ proteins can play dual roles in transcriptional regulation depending on the target gene; some promoters are activated (45,47,57), while others are repressed (44,46).

MAZ also plays a role in transcription termination. In particular, MAZ can repress transcriptional elongation of *MYB* through its binding to a G-quadruplex structure formed by a GGA repeat region (*GC* box) located in its 5′UTR (29). It therefore seems that MAZ plays a dual role in *MYB* expression regulation by either activating or terminating transcription through its binding to the *E2F/MAZ* element in the promoter or to the G-quadruplex structure, respectively. Net changes in *MYB* expression might therefore be regulated through preferential recruitment of MAZ to the promoter or to the GGA repeat region. The interaction of other transcription factors with MAZ or their binding to their corresponding elements in the *MYB* gene may potentially increase MAZ affinity for one of its binding sites and therefore promote gene activation or repression. Forced expression of a non-specified MAZ isoform in HEK-293 cells decreased the activity of a transfected *MYB* regulatory region that included the promoter and its downstream GGA repeat region (29). In contrast, using a similar regulatory region in primary T lymphocytes, we have shown that the *E2F/MAZ* site in the *MYB* promoter is required for its activation. Moreover, while *MAZ* knockdown failed to affect *MYB* promoter regulation in HEK-293 cells (29), we have shown that *MAZ* silencing in primary T lymphocytes greatly impaired *MYB* mRNA induction during the exit from quiescence. The forced expression of a given MAZ isoform in HEK-293 cells might account for the discrepant result observed in *MYB* regulation. Supporting this hypothesis, MAZ-1 and MAZ-2 have shown opposing effects on the regulation of a reporter vector driven by three tandem copies of the MAZ site in the *SAA* promoter (25). However, using a reporter driven by two tandem copies of the *MYB E2F/MAZ* site, we have shown that MAZ-1, MAZ-2 and MAZ-2s activated transcription. Alternatively, our results might suggest that the net effect of MAZ on *MYB* regulation depends on the cell type or on the cell cycle status (continuously cycling cells versus cells exiting from quiescence), rather than on the MAZ isoform expressed.

MAZ-1, MAZ-2 and MAZ-3 have been shown to regulate transcription of various genes (24–26) and we show now that MAZ-1, MAZ-2 and MAZ-2s bind the *MYB* combined *E2F/MAZ* site and activate transcription through this element. Moreover, we show that MAZ proteins overcome RB family-mediated transcriptional repression. In addition, we have obtained evidence suggesting the existence of an additional MAZ isoform, MAZ-1s. The use of the MAZ antibody M-13, raised against a peptide from the carboxy-terminal end of MAZ-1 and MAZ-3, in immunoblot assays identified a major protein of ∼50 kDa, the expected size of MAZ-1, in HEK-293T cells transfected with MAZ-1. However, an additional protein of ∼30 kDa was clearly detected also with this antibody in control cells and the signal was even stronger in MAZ-1 transfected cells. Whether this protein is the result of a new alternatively spliced isoform, a cleavage product of MAZ-1 or the product of an internal translation initiation site remains to be elucidated.

Our UV cross-linking analysis showed that Myb-sp contained a protein of ∼30 kDa, which is similar to the relative mobility of MAZ-1s and MAZ-2s. Mass spectrometry analysis of this protein revealed six peptides common to all MAZ isoforms and an additional peptide that was present only in MAZ-2 and MAZ-2s. These results might suggest that MAZ-2s is the protein present in Myb-sp, but the inhibition of Myb-sp complex formation in EMSA assays by an antibody to MAZ-1/MAZ-3 (M-13) and the reactivity of this antibody to a short MAZ-1 isoform (or degradation product) of ∼30 kDa, rather support the notion that at least MAZ-1 and MAZ-2 (or their short isoforms) can regulate *MYB* expression through the combined *E2F/MAZ* site.

MAZ phosphorylation by various kinases regulates its activity. In particular, its phosphorylation at S460 by casein kinase II (CKII) increases MAZ DNA-binding activity (33). MAZ phosphorylation at T72 by the mitogen-activated protein kinase signaling pathway (58) or at S187 and T386 by protein kinase A (59) also increases MAZ activity. We could not assess MAZ phosphorylation at T72, S187 or T386 during the exit from quiescence, but we have found that MAZ S460 phosphorylation was markedly induced as early as 1 and 3 h after entry in the cell cycle. We therefore propose a model by which phosphorylation-mediated MAZ activation early after the exit from quiescence increases MAZ binding to the *MYB* promoter, likely through the E2F/MAZ element, alleviating DREAM-mediated repression until the phosphorylation-mediated inactivation of RB family members late in G1.

SUPPLEMENTARY DATA

Supplementary Data are available at NAR Online.

ACKNOWLEDGEMENTS

We thank the Madrid Blood Donor Centre for supplying Buffy coats and D. Trono's lab for plasmids. The following reagent was obtained through the AIDS Research and Reference Reagent Program, Division of AIDS, NIAID, NIH: Human rIL-2 from Dr Maurice Gately, Hoffmann—La Roche Inc. The proteomic analysis was performed in the proteomics facility of the Spanish National Center for Biotechnology (CNB-CSIC) that belongs to ProteoRed, PRB2-ISCIII.

FUNDING

Spanish Ministerio de Economía, Industria y Competitividad [SAF2013–45258P to M.R.C., SAF2014–52737P to T.I.]; Instituto de Salud Carlos III [FIS PI12/0056 to J.A., CIBERNED to T.I.]; Spanish AIDS Research Network [RD16CIII/0002/0001 to J.A.]; FEDER funds (in part); Spanish National Center for Biotechnology [PT13/0001]. Funding for open access charge: Spanish Ministerio de Economía, Industria y Competitividad [SAF2013–45258P].
Conflict of interest statement. None declared.

REFERENCES

1. Pattabiraman,D.R. and Gonda,T.J. (2013) Role and potential for therapeutic targeting of MYB in leukemia. *Leukemia*, **27**, 269–277.
2. Ramsay,R.G. and Gonda,T.J. (2008) MYB function in normal and cancer cells. *Nat. Rev. Cancer*, **8**, 523–534.
3. Zhou,Y. and Ness,S.A. (2011) Myb proteins: angels and demons in normal and transformed cells. *Front. Biosci. (Landmark Ed.)*, **16**, 1109–1131.
4. Friedman,A.D. (2002) Runx1, c-Myb, and C/EBPalpha couple differentiation to proliferation or growth arrest during hematopoiesis. *J. Cell Biochem.*, **86**, 624–629.
5. Campanero,M.R., Armstrong,M. and Flemington,E. (1999) Distinct cellular factors regulate the c-myb promoter through its E2F element. *Mol. Cell. Biol.*, **19**, 8442–8450.
6. Sala,A., Nicolaides,N.C., Engelhard,A., Bellon,T., Lawe,D.C., Arnold,A., Grana,X., Giordano,A. and Calabretta,B. (1994) Correlation between E2F-1 requirement in the S phase and E2F-1 transactivation of cell cycle-related genes in human cells. *Cancer Res.*, **54**, 1402–1406.
7. Chen,H.Z., Tsai,S.Y. and Leone,G. (2009) Emerging roles of E2Fs in cancer: an exit from cell cycle control. *Nat. Rev. Cancer*, **9**, 785–797.
8. Dick,F.A. (2007) Structure-function analysis of the retinoblastoma tumor suppressor protein - is the whole a sum of its parts? *Cell Div*, **2**, 26.
9. Sadasivam,S. and DeCaprio,J.A. (2013) The DREAM complex: master coordinator of cell cycle-dependent gene expression. *Nat. Rev. Cancer*, **13**, 585–595.
10. Litovchick,L., Sadasivam,S., Florens,L., Zhu,X., Swanson,S.K., Velmurugan,S., Chen,R., Washburn,M.P., Liu,X.S. and DeCaprio,J.A. (2007) Evolutionarily conserved multisubunit RBL2/p130 and E2F4 protein complex represses human cell cycle-dependent genes in quiescence. *Mol. Cell*, **26**, 539–551.
11. Stern,J.B. and Smith,K.A. (1986) Interleukin-2 induction of T-cell G1 progression and c-myb expression. *Science*, **233**, 203–206.
12. Thompson,C.B., Challoner,P.B., Neiman,P.E. and Groudine,M. (1986) Expression of the c-myb proto-oncogene during cellular proliferation. *Nature*, **319**, 374–380.
13. Alvaro-Blanco,J., Martinez-Gac,L., Calonge,E., Rodriguez-Martinez,M., Molina-Privado,I., Redondo,J.M., Alcami,J., Flemington,E.K. and Campanero,M.R. (2009) A novel factor distinct from E2F mediates C-MYC promoter activation through its E2F element during exit from quiescence. *Carcinogenesis*, **30**, 440–448.
14. Lahm,H.W. and Stein,S. (1985) Characterization of recombinant human interleukin-2 with micromethods. *J. Chromatogr.*, **326**, 357–361.
15. Cantrell,D.A. and Smith,K.A. (1984) The interleukin-2 T-cell system: a new cell growth model. *Science*, **224**, 1312–1316.
16. Campanero,M.R., Herrero,A. and Calvo,V. (2008) The histone deacetylase inhibitor trichostatin A induces GADD45 gamma expression via Oct and NF-Y binding sites. *Oncogene*, **27**, 1263–1272.
17. Vizcaino,J.A., Csordas,A., del-Toro,N., Dianes,J.A., Griss,J., Lavidas,I., Mayer,G., Perez-Riverol,Y., Reisinger,F., Ternent,T. *et al.*

(2016) 2016 update of the PRIDE database and its related tools. *Nucleic Acids Res.*, **44**, D447–D456.
18. Campanero,M.R., Armstrong,M.I. and Flemington,E.K. (2000) CpG methylation as a mechanism for the regulation of E2F activity. *Proc. Natl. Acad. Sci. U.S.A.*, **97**, 6481–6486.
19. Nicolaides,N.C., Gualdi,R., Casadevall,C., Manzella,L. and Calabretta,B. (1991) Positive autoregulation of c-myb expression via Myb binding sites in the 5′ flanking region of the human c-myb gene. *Mol. Cell. Biol.*, **11**, 6166–6176.
20. Campanero,M.R. and Flemington,E.K. (1997) Regulation of E2F through ubiquitin-proteasome-dependent degradation: stabilization by the pRB tumor suppressor protein. *Proc. Natl. Acad. Sci. U.S.A.*, **94**, 2221–2226.
21. Alcami,J., Lain de Lera,T., Folgueira,L., Pedraza,M.A., Jacque,J.M., Bachelerie,F., Noriega,A.R., Hay,R.T., Harrich,D., Gaynor,R.B. *et al.* (1995) Absolute dependence on kappa B responsive elements for initiation and Tat-mediated amplification of HIV transcription in blood CD4 T lymphocytes. *EMBO J.*, **14**, 1552–1560.
22. Molina-Privado,I., Jimenez,P.R., Montes-Moreno,S., Chiodo,Y., Rodriguez-Martinez,M., Sanchez-Verde,L., Iglesias,T., Piris,M.A. and Campanero,M.R. (2012) E2F4 plays a key role in Burkitt lymphoma tumorigenesis. *Leukemia*, **26**, 2277–2285.
23. Molina-Privado,I., Rodriguez-Martinez,M., Rebollo,P., Martin-Perez,D., Artiga,M.J., Menarguez,J., Flemington,E.K., Piris,M.A. and Campanero,M.R. (2009) E2F1 expression is deregulated and plays an oncogenic role in sporadic Burkitt's lymphoma. *Cancer Res.*, **69**, 4052–4058.
24. Bossone,S.A., Asselin,C., Patel,A.J. and Marcu,K.B. (1992) MAZ, a zinc finger protein, binds to c-MYC and C2 gene sequences regulating transcriptional initiation and termination. *Proc. Natl. Acad. Sci. U.S.A.*, **89**, 7452–7456.
25. Ray,B.K., Murphy,R., Ray,P. and Ray,A. (2002) SAF-2, a splice variant of SAF-1, acts as a negative regulator of transcription. *J. Biol. Chem.*, **277**, 46822–46830.
26. Ray,A., Dhar,S., Shakya,A., Ray,P., Okada,Y. and Ray,B.K. (2009) SAF-3, a novel splice variant of the SAF-1/MAZ/Pur-1 family, is expressed during inflammation. *FEBS J.*, **276**, 4276–4286.
27. Strausberg,R.L., Feingold,E.A., Grouse,L.H., Derge,J.G., Klausner,R.D., Collins,F.S., Wagner,L., Shenmen,C.M., Schuler,G.D., Altschul,S.F. *et al.* (2002) Generation and initial analysis of more than 15,000 full-length human and mouse cDNA sequences. *Proc. Natl. Acad. Sci. U.S.A.*, **99**, 16899–16903.
28. Ray,A., Kumar,D., Ray,P. and Ray,B.K. (2004) Transcriptional activity of serum amyloid A-activating factor-1 is regulated by distinct functional modules. *J. Biol. Chem.*, **279**, 54637–54646.
29. Palumbo,S.L., Memmott,R.M., Uribe,D.J., Krotova-Khan,Y., Hurley,L.H. and Ebbinghaus,S.W. (2008) A novel G-quadruplex-forming GGA repeat region in the c-myb promoter is a critical regulator of promoter activity. *Nucleic Acids Res.*, **36**, 1755–1769.
30. Martinez-Gac,L., Marques,M., Garcia,Z., Campanero,M.R. and Carrera,A.C. (2004) Control of cyclin G2 mRNA expression by forkhead transcription factors: novel mechanism for cell cycle control by phosphoinositide 3-kinase and forkhead. *Mol. Cell. Biol.*, **24**, 2181–2189.
31. Smith,E.J., Leone,G., DeGregori,J., Jakoi,L. and Nevins,J.R. (1996) The accumulation of an E2F-p130 transcriptional repressor distinguishes a G0 cell state from a G1 cell state. *Mol. Cell. Biol.*, **16**, 6965–6976.
32. Kaelin,W.G. Jr, Krek,W., Sellers,W.R., DeCaprio,J.A., Ajchenbaum,F., Fuchs,C.S., Chittenden,T., Li,Y., Farnham,P.J., Blanar,M.A. *et al.* (1992) Expression cloning of a cDNA encoding a retinoblastoma-binding protein with E2F-like properties. *Cell*, **70**, 351–364.
33. Tsutsui,H., Geltinger,C., Murata,T., Itakura,K., Wada,T., Handa,H. and Yokoyama,K.K. (1999) The DNA-binding and transcriptional activities of MAZ, a myc-associated zinc finger protein, are regulated by casein kinase II. *Biochem. Biophys. Res. Commun.*, **262**, 198–205.
34. Bellon,T., Perrotti,D. and Calabretta,B. (1997) Granulocytic differentiation of normal hematopoietic precursor cells induced by transcription factor PU.1 correlates with negative regulation of the c-myb promoter. *Blood*, **90**, 1828–1839.
35. Guerra,J., Withers,D.A. and Boxer,L.M. (1995) Myb binding sites mediate negative regulation of c-myb expression in T-cell lines. *Blood*, **86**, 1873–1880.
36. Lauder,A., Castellanos,A. and Weston,K. (2001) c-Myb transcription is activated by protein kinase B (PKB) following interleukin 2 stimulation of Tcells and is required for PKB-mediated protection from apoptosis. *Mol. Cell. Biol.*, **21**, 5797–5805.
37. Muller,H., Bracken,A.P., Vernell,R., Moroni,M.C., Christians,F., Grassilli,E., Prosperini,E., Vigo,E., Oliner,J.D. and Helin,K. (2001) E2Fs regulate the expression of genes involved in differentiation, development, proliferation, and apoptosis. *Genes Dev.*, **15**, 267–285.
38. Nicolaides,N.C., Correa,I., Casadevall,C., Travali,S., Soprano,K.J. and Calabretta,B. (1992) The Jun family members, c-Jun and JunD, transactivate the human c-myb promoter via an Ap1-like element. *J. Biol. Chem.*, **267**, 19665–19672.
39. Kelly,K., Cochran,B.H., Stiles,C.D. and Leder,P. (1983) Cell-specific regulation of the c-myc gene by lymphocyte mitogens and platelet-derived growth factor. *Cell*, **35**, 603–610.
40. Kennedy,G.C. and Rutter,W.J. (1992) Pur-1, a zinc-finger protein that binds to purine-rich sequences, transactivates an insulin promoter in heterologous cells. *Proc. Natl. Acad. Sci. U.S.A.*, **89**, 11498–11502.
41. Ray,A. and Ray,B.K. (1996) A novel cis-acting element is essential for cytokine-mediated transcriptional induction of the serum amyloid A gene in nonhepatic cells. *Mol. Cell. Biol.*, **16**, 1584–1594.
42. Pyrc,J.J., Moberg,K.H. and Hall,D.J. (1992) Isolation of a novel cDNA encoding a zinc-finger protein that binds to two sites within the c-myc promoter. *Biochemistry*, **31**, 4102–4110.
43. Her,S., Bell,R.A., Bloom,A.K., Siddall,B.J. and Wong,D.L. (1999) Phenylethanolamine N-methyltransferase gene expression. Sp1 and MAZ potential for tissue-specific expression. *J. Biol. Chem.*, **274**, 8698–8707.
44. Karantzoulis-Fegaras,F., Antoniou,H., Lai,S.L., Kulkarni,G., D'Abreo,C., Wong,G.K., Miller,T.L., Chan,Y., Atkins,J., Wang,Y. *et al.* (1999) Characterization of the human endothelial nitric-oxide synthase promoter. *J. Biol. Chem.*, **274**, 3076–3093.
45. Parks,C.L. and Shenk,T. (1996) The serotonin 1a receptor gene contains a TATA-less promoter that responds to MAZ and Sp1. *J. Biol. Chem.*, **271**, 4417–4430.
46. Song,J., Ugai,H., Ogawa,K., Wang,Y., Sarai,A., Obata,Y., Kanazawa,I., Sun,K., Itakura,K. and Yokoyama,K.K. (2001) Two consecutive zinc fingers in Sp1 and in MAZ are essential for interactions with cis-elements. *J. Biol. Chem.*, **276**, 30429–30434.
47. Williams,L.J. and Abou-Samra,A.B. (2000) The transcription factors SP1 and MAZ regulate expression of the parathyroid hormone/parathyroid hormone-related peptide receptor gene. *J. Mol. Endocrinol.*, **25**, 309–319.
48. Song,J., Murakami,H., Tsutsui,H., Tang,X., Matsumura,M., Itakura,K., Kanazawa,I., Sun,K. and Yokoyama,K.K. (1998) Genomic organization and expression of a human gene for Myc-associated zinc finger protein (MAZ). *J. Biol. Chem.*, **273**, 20603–20614.
49. Duncan,D.D., Stupakoff,A., Hedrick,S.M., Marcu,K.B. and Siu,G. (1995) A Myc-associated zinc finger protein binding site is one of four important functional regions in the CD4 promoter. *Mol. Cell. Biol.*, **15**, 3179–3186.
50. Ray,A., Fields,A.P. and Ray,B.K. (2000) Activation of transcription factor SAF involves its phosphorylation by protein kinase C. *J. Biol. Chem.*, **275**, 39727–39733.
51. Uchida,S., Tanaka,Y., Ito,H., Saitoh-Ohara,F., Inazawa,J., Yokoyama,K.K., Sasaki,S. and Marumo,F. (2000) Transcriptional regulation of the CLC-K1 promoter by myc-associated zinc finger protein and kidney-enriched Kruppel-like factor, a novel zinc finger repressor. *Mol. Cell. Biol.*, **20**, 7319–7331.
52. Cogoi,S., Shchekotikhin,A.E. and Xodo,L.E. (2014) HRAS is silenced by two neighboring G-quadruplexes and activated by MAZ, a zinc-finger transcription factor with DNA unfolding property. *Nucleic Acids Res.*, **42**, 8379–8388.
53. Liu,B., Ma,A., Zhang,F., Wang,Y., Li,Z., Li,Q., Xu,Z. and Zheng,Y. (2016) MAZ mediates the cross-talk between CT-1 and NOTCH1 signaling during gliogenesis. *Sci. Rep.*, **6**, 21534.
54. Daheron,L., Salmeron,S., Patri,S., Brizard,A., Guilhot,F., Chomel,J.C. and Kitzis,A. (1998) Identification of several genes differentially expressed during progression of chronic myelogenous leukemia. *Leukemia*, **12**, 326–332.

55. Sipe,J.D. (1994) Amyloidosis. *Crit. Rev. Clin. Lab. Sci.*, **31**, 325–354.
56. Uhlar,C.M. and Whitehead,A.S. (1999) Serum amyloid A, the major vertebrate acute-phase reactant. *Eur. J. Biochem.*, **265**, 501–523.
57. Parks,C.L. and Shenk,T. (1997) Activation of the adenovirus major late promoter by transcription factors MAZ and Sp1. *J. Virol.*, **71**, 9600–9607.
58. Ray,A., Yu,G.Y. and Ray,B.K. (2002) Cytokine-responsive induction of SAF-1 activity is mediated by a mitogen-activated protein kinase signaling pathway. *Mol. Cell. Biol.*, **22**, 1027–1035.
59. Ray,A., Ray,P., Guthrie,N., Shakya,A., Kumar,D. and Ray,B.K. (2003) Protein kinase A signaling pathway regulates transcriptional activity of SAF-1 by unmasking its DNA-binding domains. *J. Biol. Chem.*, **278**, 22586–22595.